

Incommensurate Magnetic Correlations in $\text{La}_{1.8}\text{Sr}_{0.2}\text{NiO}_4$

S. M. Hayden,⁽¹⁾ G. H. Lander,⁽²⁾ J. Zarestky,⁽³⁾ P. J. Brown,⁽⁴⁾ C. Stassis,⁽³⁾ P. Metcalf,⁽⁵⁾ and J. M. Honig⁽⁵⁾

⁽¹⁾*H. H. Wills Physics Laboratory, University of Bristol, Tyndall Avenue, Bristol BS8 1TL, United Kingdom*

⁽²⁾*Commission of the European Communities, Joint Research Centre, Postfach 2340, D-7500 Karlsruhe, Germany*

⁽³⁾*Ames Laboratory and Department of Physics, Iowa State University, Iowa 50011*

⁽⁴⁾*Institut Laue-Langevin, BP 156X, 38042 Grenoble, France*

⁽⁵⁾*Department of Chemistry, Purdue University, West Lafayette, Indiana 47907*

(Received 17 June 1991)

Neutron scattering experiments on an insulating single crystal of $\text{La}_{1.8}\text{Sr}_{0.2}\text{NiO}_4$ show the presence of strong two-dimensional incommensurate magnetic correlations in the NiO_2 planes. At low temperatures, $T=2$ K, these exist on time scales $\tau > 10^{-11}$ s. The typical side length of the correlated regions in the direction parallel to the incommensurate modulation is equal to the average spacing between strontium atoms.

PACS numbers: 75.25.+z, 64.70.Kb, 75.30.Ds

The discovery of high- T_c superconductivity [1] has revived interest in the relationship between the metal-insulator transition and magnetic behavior in strongly correlated electron systems [2]. The interplay between these phenomena and superconductivity remains a subject of considerable debate [3]. It is well known that La_2CuO_4 is an antiferromagnetic Mott insulator [4], and substitution of La with Sr or Ba leads to a suppression of the antiferromagnetic ordering followed by a metal-insulator transition and superconductivity [5]. We describe here an investigation of the effect of Sr substitution on the isostructural compound La_2NiO_4 . The stoichiometric compound is also an antiferromagnetic insulator [6,7] which can be made metallic at low temperatures by extensive strontium substitution [8,9]. Our investigation reveals that at smaller levels of substitution the system exhibits novel two-dimensional incommensurate antiferromagnetic fluctuations.

Both stoichiometric La_2CuO_4 and La_2NiO_4 show long-range commensurate 3D magnetic order characterized by an antiferromagnetic (AF) coupling of the nearest-neighbor copper [4] or nickel [7] spins. The coupling of spins within each metal-oxygen plane is much stronger than that between spins in neighboring planes. This makes the systems behave two dimensionally in many respects. The propagation direction of the AF structure is [100] in both cases (we adopt the $Bmab$ convention $a < b < c$ in the orthorhombic phase), but the spin direction is [010] in the case of the cuprate and [100] for the nickelate. The $\text{La}_{2-x}(\text{Ba},\text{Sr})_x\text{CuO}_4$ series has been the subject of many investigations [10-12]. With doping x , the long-range order is suppressed by $x \approx 0.02$ and replaced by short-range 2D commensurate correlations with a correlation length ξ determined by the separation of the dopant atoms [5,11]. For $x > 0.02$, the material shows a metallic temperature dependence of the resistivity [5]. At larger doping levels, e.g., $x \approx 0.075$, incommensurate short-range correlations have been reported in the metallic phase [11]. These have recently

been mapped out in detail by Cheong *et al.* [13]. The maximum T_c for the superconductivity is reached for $x \approx 0.15$. $\text{La}_{2-x}\text{Sr}_x\text{NiO}_4$ can also be made to exhibit metallic behavior at low temperatures [8,9] but for much larger levels of substitution, $x \approx 1$. However, in contrast to the cuprate system, bulk superconductivity has not been found for any x . We find for $x=0.2$, in the *insulating* phase, that the 3D magnetic order is suppressed and replaced by 2D *incommensurate* correlations.

Our experiments were performed on a single crystal (0.25 cm^3) of $\text{La}_{1.8}\text{Sr}_{0.2}\text{NiO}_4$ produced at Purdue University; the method of preparation is described elsewhere [14]. The single crystal was annealed under CO-CO_2 mixtures at 1000°C for 24 h at a pressure of $\log f_{\text{O}_2}(\text{atm}) = -11.7$, while monitoring the pressure with a $\text{Y}_2\text{O}_3\text{-ZrO}_2$ oxygen transfer cell. The oxygen to nickel ratio was determined by iodometric titration to be 3.96 ± 0.06 . The absence of any additional Bragg reflections at low temperature [14] indicated that our crystal displayed no long-range 3D antiferromagnetic order. The $T=5$ K lattice parameters were $a=5.346 \text{ \AA}$, $b=5.362 \text{ \AA}$, $c=12.4 \text{ \AA}$ (in view of the small orthorhombic distortion we use a tetragonal notation; we are unable to distinguish between the [100] and [010] directions in this experiment). The magnetic susceptibility measured in a field of 0.9 T becomes very anisotropic at low temperatures, the in-plane susceptibility χ_{ab} showing a cusp at $T \approx 17$ K [14]. The low-temperature resistivity $\rho(T)$ can be described by a variable-range hopping form or simple activated form with $E_g \approx 30\text{-}50 \text{ meV}$ [8,15]. At higher temperatures, $T > 600$ K, the resistivity takes on the characteristics of a poor "metal" with $\rho \sim 0.1 \text{ } \Omega \text{ cm}$ and a slight increase of ρ with T .

Neutron scattering measurements were performed using the cold-source triple-axis spectrometer IN12 at the Institut Laue-Langevin, Grenoble. Focused pyrolytic-graphite monochromator and analyzer were used with an incident wave vector of $k_i = 1.55 \text{ \AA}^{-1}$. The main part of Fig. 1 shows a contour plot of the scattered intensity in

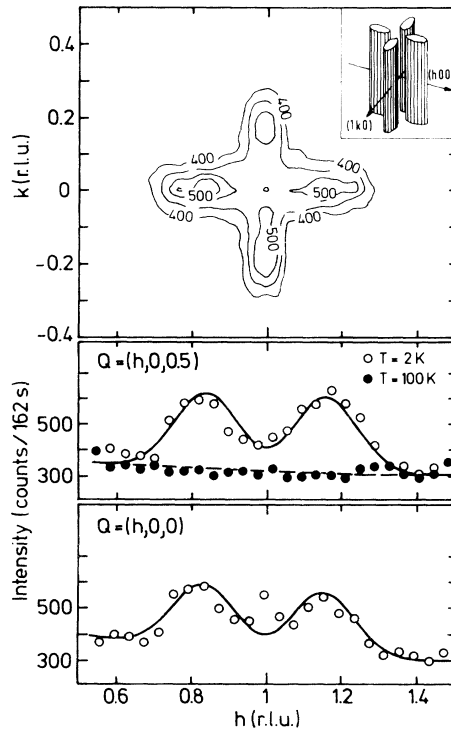


FIG. 1. Upper panel: A contour plot of the scattered intensity from $\text{La}_{1.8}\text{Sr}_{0.2}\text{NiO}_4$ in the $(hk, \frac{1}{2})$ plane around the $(1,0, \frac{1}{2})$ position for $T=2$ K. The spectrometer was set at the elastic, $\hbar\omega=0$, position and collected neutrons within an energy window of width $\Delta\hbar\omega=82$ μeV (HWHM). The Q resolution of the spectrometer is approximately a circle of radius 0.02 r.l.u. (radiation length unit). The plot was compiled from scans with a maximum separation of 0.02 r.l.u. between grid points in the central square of side 0.4 r.l.u. and 0.04 r.l.u. elsewhere. Right inset: A 3D impression of the scattering. Lower panel: $\hbar\omega=0$, $Q=(h,0,l)$ scans through the pattern for different values of l (the momentum transfer perpendicular to the basal plane). The constant amplitude of the modulation shows the two-dimensional nature of the scattering.

the $(hk, \frac{1}{2})$ plane in reciprocal space around the $(1,0, \frac{1}{2})$ position for $\hbar\omega=0$ and $T=2$ K. There is strong scattering near the four incommensurate "satellite" positions $(1 \pm \delta, 0, \frac{1}{2})$ and $(1, \pm \delta, \frac{1}{2})$. Similar patterns were observed around the $(1,0,0)$, $(1,0,1)$, and $(2,1,0)$ positions. The lower part of Fig. 1 shows $\hbar\omega=0$ scans in the $[100]$ direction (through the peaks) for different values of l . The small variation of the amplitude of the modulation with l shows the 2D nature of the correlations. We conclude the correlations are within the NiO_2 planes with little correlation between planes (just as in the doped cuprate). The intensity distribution may be described by four anisotropic Gaussian peaks centered at the positions $(1,0,l) \pm \delta$, where $\delta=(\pm\delta,0,0)$ and $(0,\pm\delta,0)$. For $T=2$ K, we obtain $|\delta|=0.160(10)$ r.l.u., $\xi_{\parallel}^{-1}=0.115(8)$ \AA^{-1} , and $\xi_{\perp}^{-1}=0.060(4)$ \AA^{-1} , where ξ_{\parallel}^{-1} and ξ_{\perp}^{-1} are the half width at half maximum (HWHM) peak widths

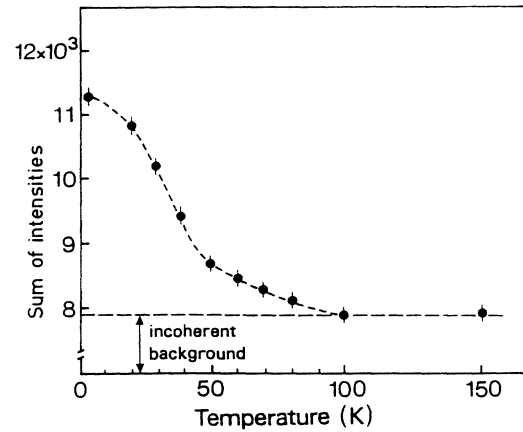


FIG. 2. The variation of the integrated intensity with temperature of a constant $\hbar\omega=0$, $Q=(h,0, \frac{1}{2})$ scan (i.e., through the center of the plot in the upper panel of Fig. 1). The total counting time was 25×162 s.

of the Gaussians in directions parallel and perpendicular to δ . The elastic resolution was $\Delta\hbar\omega=82$ μeV and $\Delta q=0.02$ \AA^{-1} (HWHM). Under the experimental conditions, the spectrometer performs an integration over a window in energy (frequency) of width $\Delta\hbar\omega=82$ μeV or $\Delta\nu=20$ GHz (HWHM). Scattering observed within this window is associated with correlations which persist on time scales longer than $\Delta\tau \approx 1/\Delta\omega \approx 10^{-11}$ s. Thus, at $T=2$ K, the sample is divided into 2D-correlated regions of typical side lengths ξ_{\parallel}^{-1} and ξ_{\perp}^{-1} ; these are frozen on time scales of $\Delta\tau$. The variation of the scattered intensity within the energy window with temperature is shown in Fig. 2. As we shall see below, the decrease of the intensity with increasing temperature is due to a decrease in the lifetime of the correlated regions: At high temperatures they exist for times much less than $\Delta\tau$ above.

We now turn to the energy dependence of the scattering. Figure 3 shows constant-energy scans for $\hbar\omega=0$ meV and $\hbar\omega=2$ meV at $T=19$ K and $T=79$ K. The lower panel shows that the modulation (as shown in Fig. 1) develops as the temperature is lowered from $T=79$ to 19 K. The upper panel shows that the modulation exists for $\hbar\omega=2$ meV and is stronger at the higher temperature, $T=79$ K. The energy spectra in Fig. 4 show the distribution of the different frequency components at $Q=(1.2,0,0)$, near the peak in the scattering. The measured intensity is proportional to the power spectrum of the fluctuating spin magnetization [16] $\langle |m(q,\omega)|^2 \rangle$ averaged over the experimental resolution, where $m(q,\omega)$ is the Fourier transform of the local spin magnetization $m(r,t)$. [We remind the reader that our experiment says nothing about the existence of infinite time correlations, which imply a nonzero value for $\langle |m(q,\omega)|^2 \rangle$.] As the temperature is lowered, the correlations move to lower frequencies with no observable change in the spatial dependence over the energy range investigated (0–2 meV). The behavior should be contrasted with a conven-

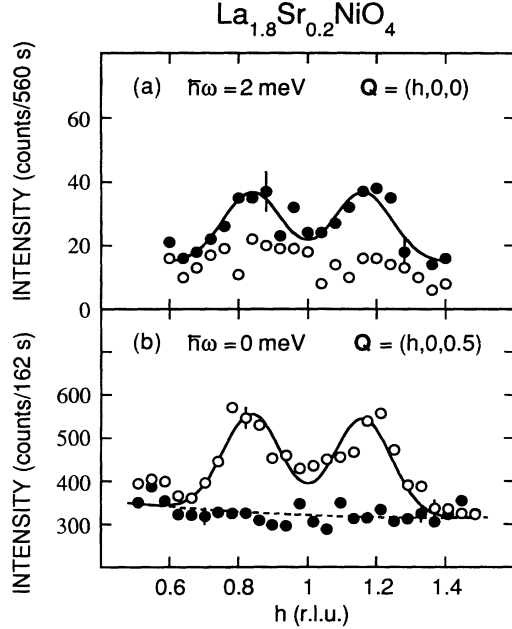


FIG. 3. The variation of the modulation with temperature (a) at finite energy transfer, $\hbar\omega = 2$ meV, and (b) at the elastic position, $\hbar\omega = 0$ meV. Open and solid circles are $T = 19$ and 79 K, respectively. The data shown in Figs. 3 and 4 have been normalized to a monitor placed in the incident beam (counting times are approximate).

tional second-order phase transition where the correlation length diverges as the system orders. In the present case there is no evidence of long-range order at temperatures as low as 2 K. The observed redistribution of scattered intensity with temperature has similarities with the behavior observed in spin glasses [17] and more recently in the $\text{La}_{2-x}(\text{Ba},\text{Sr})_x\text{CuO}_4$ system [11,12,18,19]. Detailed studies over a wide energy range have been performed on $\text{La}_{1.95}\text{Ba}_{0.05}\text{CuO}_4$ [12] and $\text{La}_{1.96}\text{Sr}_{0.04}\text{CuO}_4$ [19]. In the present experiment we concentrate on the low-energy dynamics and defer a detailed comparison of the two systems for future experiments. The observed dynamic response can be interpreted using the functional form used to analyze $\text{La}_{1.95}\text{Ba}_{0.05}\text{CuO}_4$ [12] (the form given in Ref. [19] could also be used). A spectrum characterized by a *local* response $\langle |m(0,\omega)|^2 \rangle \propto \chi''_0(\omega)[n(\omega)+1]$ was employed, where $n(\omega) = [\exp(\hbar\omega\beta) - 1]^{-1}$,

$$\chi''_0(\omega) = A\omega \int_{\Gamma_0}^{\infty} \frac{d\Gamma}{\Gamma^2 + \omega^2} = A \tan^{-1} \left(\frac{\omega}{\Gamma_0} \right),$$

$m(0,t)$ is the (fluctuating) moment on the nickel site, and the integral represents a distribution of relaxation rates with a minimum Γ_0 . In $\text{La}_{1.8}\text{Sr}_{0.2}\text{NiO}_4$, on warming from $T = 10$ to 80 K we see an increase of $\hbar\Gamma_0$ from 0.01 ± 0.04 to 0.8 ± 0.2 meV. Thus the characteristic magnetic relaxation rate increases with temperature, reducing the signal observed in the elastic window.

Our measurements show that $\text{La}_{1.8}\text{Sr}_{0.2}\text{NiO}_4$ forms regions of two-dimensionally correlated spins at low tem-

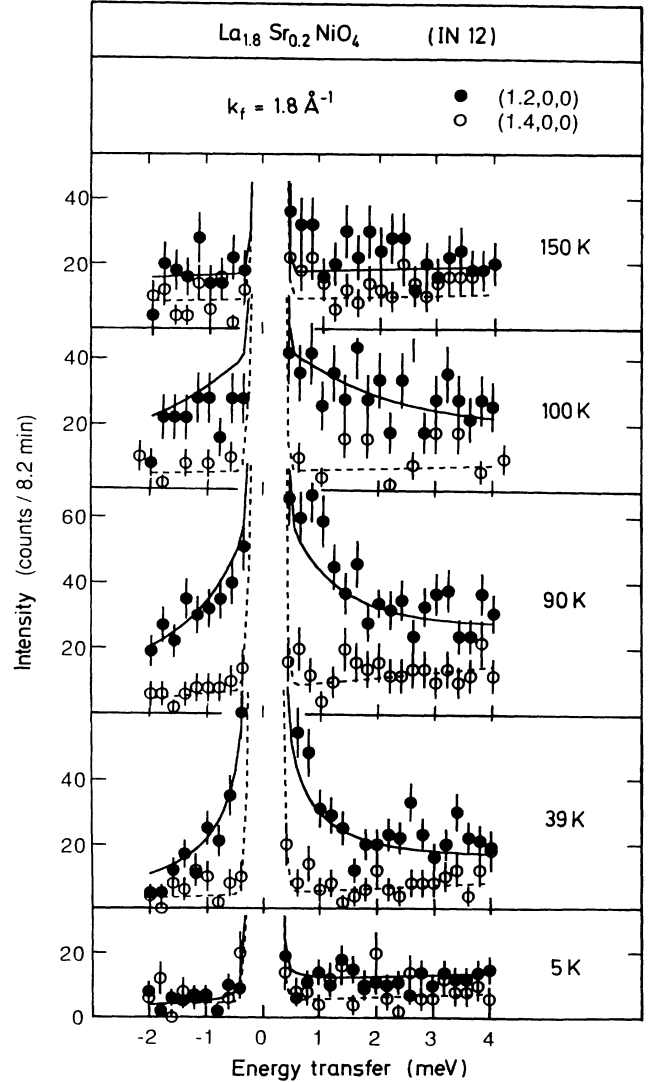


FIG. 4. Constant- Q scans at $Q = (1.2, 0, 0)$ (near peak in signal) and $Q = (1.4, 0, 0)$ (background). The scans were made with a fixed final neutron wave number $k_f = 1.8 \text{ \AA}^{-1}$. The elastic energy resolution was $130 \mu\text{eV}$ (HWHM). The solid lines are fits with the model described in the text. Values obtained for $\hbar\Gamma_0$ were 0.0 ± 0.004 (5 K), 0.031 ± 0.004 , 0.77 ± 0.20 , 0.85 ± 0.20 , and 8.0 ± 2.0 meV (150 K), respectively.

peratures. The spatial extent of these correlated regions is anisotropic: Parallel to δ , the typical side length $\xi_{\parallel} \approx 8.7 \text{ \AA}$, and perpendicular to δ , $\xi_{\perp} \approx 17 \text{ \AA}$. Assuming random substitution, the mean distance between strontium atoms (or holes) [11] is $\xi_d \approx 3.8/\sqrt{x} \approx 8.5 \text{ \AA}$. The length of the domains parallel to δ is determined by this distance with $\xi_{\parallel} \approx \xi_d$ (as is the case in the lightly doped cuprates). With the present unpolarized-neutron diffraction experiments we cannot determine unambiguously the nature of the structure within these regions. There are several possibilities broadly consistent with our observations. (i) A transverse modulation of the magnitude of the staggered moment. A purely longitudinal

modulation can be excluded because of the presence of the four satellites in Fig. 1. (ii) A spiral order arrangement in which the direction of the staggered moment rotates in the plane. Such a model [20] has been proposed in which an incommensurate modulation results from the interaction of the holes with long-wavelength AF spin waves. (iii) A structure in which the incommensurate peak results from correlations in antiphase domain boundaries. Such structures are well known in systems with competing interactions (e.g., the axial next-nearest-neighbor Ising model [21]) and have been discussed in the literature in the context of the cuprates [22,23]. Calculations [24] involving a model with a distribution of domain sizes, with mean ξ , can successfully reproduce the essential features of the observed scattering pattern.

In summary, we have shown that the substitution of bivalent La by trivalent Sr in the insulating antiferromagnet La_2NiO_4 leads to magnetic correlations peaked at the wave vectors $\mathbf{Q}=(\pi\pm\delta\pi,\pi\pm\delta\pi)$ and $(\pi\pm\delta\pi,\pi\mp\delta\pi)$ with $\delta=0.16$ for $x=0.2$ [we use here the *square-lattice antiferromagnet notation*; in this notation commensurate order would correspond to (π,π)]. As the temperature is lowered, the lifetime of the correlated regions increases. At the lowest temperatures investigated, $T=2$ K, the correlations exist on time scales τ longer than the experimental resolution $\Delta\tau\approx 10^{-11}$ s, but drop for $T=80$ K to $\tau\approx 10^{-12}$ s. The microscopic effect of Sr substitution in the nickelate is unclear. Clearly, the Sr atoms modify the interactions in the system: This may be through a local mechanism or by donation of a hole to the NiO_2 plane which then alters the superexchange coupling between Ni spins. Short-range incommensurate magnetic correlations have also been reported in the $\text{La}_{2-x}\text{Sr}_x\text{CuO}_4$ system with the same structure [11,13]. There are important differences between the two systems: In the nickelate ($\text{La}_{1.8}\text{Sr}_{0.2}\text{NiO}_4$) we are some way from the metal-insulator transition, i.e., in the large on-site repulsion limit; and the cuprate ($\text{La}_{1.925}\text{Sr}_{0.075}\text{CuO}_4$) is metallic. However, we note the very similar values for $|\delta|$ in the cuprate and nickelate systems for equivalent doping levels. In contrast to the nickelate, however, the correlations in the cuprate [13] are found to be peaked at the wave vectors $\mathbf{Q}=(\pi,\pi\pm\delta\pi)$ and $(\pi\pm\delta\pi,\pi)$. The difference between the two results is intriguing and must be explained by any theory describing the magnetic correlations in these systems.

We gratefully acknowledge Gabe Aeppli for his guidance especially during the early stages of the experiment and useful discussions with Mike Gunn, Balazs Gyorffy, and John Wilson. Work at Purdue is sponsored by the National Science Foundation and that at Ames Laboratory by the Department of Energy.

[1] J. G. Bednorz and K. Müller, Z. Phys. B **189**, 189 (1986).

[2] P. W. Anderson, Science **235**, 1196 (1987).

[3] See, for example, *High Temperature Superconductivity*:

Proceedings, Proceedings of the Los Alamos Symposium, edited by K. S. Bedell *et al.* (Addison-Wesley, Reading, MA, 1990).

- [4] D. Vaknin, S. K. Sinha, D. E. Moncton, D. C. Johnston, J. M. Newsam, C. R. Safinya, and H. E. King, Phys. Rev. Lett. **58**, 2802 (1987).
- [5] H. Takagi, T. Ido, S. Ishibashi, M. Uota, S. Uchida, and Y. Tokura, Phys. Rev. B **40**, 2254 (1989).
- [6] D. J. Buttrey, J. M. Honig, and C. N. R. Rao, J. Solid State Chem. **64**, 287 (1986).
- [7] G. Aeppli and D. J. Buttrey, Phys. Rev. Lett. **61**, 203 (1988).
- [8] Y. Takeda, R. Kanno, M. Sakano, O. Yamamoto, M. Takano, Y. Bando, H. Akinaga, K. Takita, and J. B. Goodenough, Mater. Res. Bull. **25**, 293 (1990).
- [9] R. J. Cava, B. Batlogg, T. T. Palstra, J. J. Krajewski, W. F. Peck, A. P. Ramirez, and L. W. Rupp, Phys. Rev. B **43**, 1229 (1991).
- [10] Y. Endoh, K. Yamada, R. J. Birgeneau, D. R. Gabbe, H. P. Jenssen, M. A. Kastner, C. J. Peters, P. J. Picone, T. R. Thurston, J. M. Tranquada, G. Shirane, Y. Hidaka, M. Oda, Y. Enomoto, M. Suzuki, and T. Murakami, Phys. Rev. B **37**, 7443 (1988).
- [11] T. R. Thurston, R. J. Birgeneau, M. A. Kastner, N. W. Preyer, G. Shirane, Y. Fujii, K. Yamada, Y. Endoh, K. Kakurai, M. Matsuda, Y. Hidaka, and T. Murakami, Phys. Rev. B **40**, 4585 (1989).
- [12] S. M. Hayden, G. Aeppli, H. Mook, D. Rytz, M. F. Hundley, and Z. Fisk, Phys. Rev. Lett. **66**, 821 (1991).
- [13] S.-W. Cheong, G. Aeppli, T. E. Mason, H. Mook, S. M. Hayden, P. C. Canfield, Z. Fisk, K. N. Clausen, and J. L. Martinez, Phys. Rev. Lett. **67**, 1791 (1991).
- [14] G. H. Lander, P. J. Brown, C. Stassis, P. Gopalan, J. Spalek, and G. Honig, Phys. Rev. B **43**, 448 (1991).
- [15] S. A. Hoffman, C. Venkatraman, S. N. Ehrlich, S. M. Durbin, and G. L. Liedl, Phys. Rev. B **43**, 7852 (1991).
- [16] Neutron scattering measures only the component of $\mathbf{m}(\mathbf{q},\omega)$ perpendicular to $\mathbf{Q}=\mathbf{k}_i-\mathbf{k}_f$. The quantity $\langle|\mathbf{m}(\mathbf{q},\omega)|^2\rangle$ is the Fourier transform of the *unsymmetrized* autocorrelation function $V^{-1}\int d^3r'\langle\mathbf{m}(\mathbf{r}',0)\times\mathbf{m}(\mathbf{r}'+\mathbf{r},t)\rangle$. For more details, see S. W. Lovesey, *Theory of Neutron Scattering from Condensed Matter* (Oxford Univ. Press, Oxford, 1984).
- [17] A. P. Murani, J. Phys. (Paris), Colloq. **39**, C6-1517 (1978).
- [18] D. Harshman, G. Aeppli, G. P. Espinosa, A. S. Cooper, J. P. Remeika, E. J. Ansaldo, T. M. Riseman, D. Li. Williams, D. R. Noakes, B. Ellman, and T. F. Rosenbaum, Phys. Rev. B **38**, 852 (1988).
- [19] B. Keimer, R. J. Birgeneau, A. Cassanho, Y. Endoh, R. W. Erwin, M. A. Kastner, and G. Shirane, Phys. Rev. Lett. **67**, 1930 (1991).
- [20] B. I. Shraiman and E. D. Siggia, Phys. Rev. Lett. **61**, 467 (1988).
- [21] W. Selke, Phys. Rep. **170**, 213-264 (1988).
- [22] H. J. Schulz, J. Phys. (Paris) **50**, 2833 (1989).
- [23] A. Aharony, R. J. Birgeneau, A. Coniglio, M. A. Kastner, and H. E. Stanley, Phys. Rev. Lett. **60**, 1330 (1988).
- [24] P. J. Brown, S. M. Hayden, G. H. Lander, J. Zarestky, C. Stassis, P. Metcalf, and J. M. Honig, in Proceedings of the International Conference on Neutron Scattering, Oxford, 1991 [Physica B (to be published)].